Impact of Low-Energy Response to Nuclear Recoils in Dark Matter Detectors

D.-M. Mei,[1,2,*] W.-Z. Wei,[1,†] and L. Wang[1,‡]

[1] *Department of Physics, The University of South Dakota, Vermillion, South Dakota 57069*
[2] *College of Physics, Yangtz River University, Jingzhou 434023, China*

We report an absolute energy response function to electronic and nuclear recoils for germanium and liquid xenon detectors. As a result, we show that the detection energy threshold of nuclear recoils for a dual-phase xenon detector can be ∼ 6.8 keV for a given number of detectable photoelectrons. We evaluate the average energy expended per electron-hole pair to be ∼8.9 eV, which sets a detection energy threshold of ∼4.5 keV for a germanium detector at 50 mini-Kelvin at 69 volts with a primary phonon frequency of 2 THz. The Fano factors of nuclear and electronic recoils that constrain the capability for discriminating nuclear recoils below 2-3 keV recoil energy for both technologies are different.

PACS numbers: 95.35.+d, 95.30.Cq, 07.05.Tp, 29.40.Wk

arXiv:1512.00694v1 [physics.ins-det] 2 Dec 2015

Observations from the 1930s [1] led to the idea of dark matter, more recent observations [2, 3] lead to the contemporary and shocking revelation that 96% of the matter and energy in the universe neither emits nor absorbs electromagnetic radiation. A popular candidate for dark matter is the WIMP (Weakly Interacting Massive Particle), a particle with mass thought to be comparable to heavy nuclei, but with a feeble and extremely short-range interaction with atomic nuclei. Theories involving Supersymmetry (SUSY), which are being tested at the Large Hadron Collider [4], naturally imply a particle that could be the WIMP [5]. While WIMPs appear to collide with atomic nuclei very rarely, they would cause atoms to recoil at a velocity several thousand times the speed of sound when they do interact [6]. Direct detection of WIMPs requires the ability to observe low-energy recoils and discriminate electronic recoils originating from background events from nuclear recoils induced by WIMPs.

The detector response to low-energy recoils can be described as $E_{eff} = Y(E_r) \times E_r$, where $Y(E_r)$ is the so called ionization efficiency. For electronic recoils, $Y(E_r) = 1$, while for nuclear recoils, $Y(E_r)$ is a function of the nuclear recoil energy [7]. For a given experiment, the visible energy can be expressed as

$$E_{vis} = \frac{\alpha}{1+\beta\frac{dE_{eff}}{dx}} E_{eff}, \tag{1}$$

where α and β can be determined both theoretically or experimentally using known energy sources while $\frac{dE_{eff}}{dx}$ is given by a theoretical calculation [8]. Eq.(1) is in a form of Birks' law [9] that takes into account the reduction of visible energy due to the recombination of electron-hole (e-h) pairs or the reduction of scintillation yield along a high-density ionization track. This is to say that the reduction of visible energy is only a function of ionization density regardless of particle type. For electronic recoils, in the case in which the product of $\beta\frac{dE_r}{dx}$ is insignificant, E_{vis} is a linear function of E_r. Otherwise, E_{vis} may not be a linear function of E_r if the product of $\beta\frac{dE_r}{dx}$ is significant. In the case of nuclear recoils, Eq.(1) becomes

$$E_{vis} = \frac{\alpha}{1+\beta\frac{dE_{eff}}{dx}} \times Y(E_r) \times E_r. \tag{2}$$

Because this depends on the product of $\beta\frac{dE_{eff}}{dx}$, the further reduction of visible energy in addition to $Y(E_r)$ needs to be taken into account. In the case of liquid xenon, E_{vis} is evaluated by many authors [8, 10–17] including a data-driven model [18–21]. Note that E_{vis} is usually calibrated using gamma-ray sources and by assuming the entire energy from well-known gamma-ray energies is detectable. This type of calibration is a relative calibration because the real measurable energy for a given detector can be much smaller than the total energy deposition from a given gamma energy. This is because a large fraction of deposited energy contributes to the creation of phonons due to the requirement of momentum conservation in the energy deposition process. This fraction of energy cannot be measured by any generic ionization or scintillation detector, which can only measure the real energy to be the fraction of energy that creates e-h pairs and direct excitation, $E_{real} = \frac{E_g}{\varepsilon} \times E_{vis}$, where E_g is the band gap energy for a given target, and ε is the average energy required to produce an e-h pair.

In a germanium ionization detector, the detectable charge is proportional to the number of e-h pairs, $N_Q = \frac{E}{\varepsilon}$, created by an incoming particle with energy deposition of E, where $\varepsilon = E_g + 2E_f + rE_R$ [22] with E_g the band gap energy, E_f the final retained energy less than E_g for e-h pairs, r the number of phonons created per e-h pair, and E_R the average energy per phonon. Note that rE_R is temperature dependent. For a given temperature, ε can be a constant down to very low energy [23]. Therefore, we expect that the energy response function is an excellent linear function [24].

In a dual-phase xenon detector, $\varepsilon = (1.13 + 0.9\frac{N_{ex}}{N_i} + 0.48)E_g$ [25], where $\frac{N_{ex}}{N_i}$ is the ratio of direct excitation to ionization per energy deposition, which is energy de-

*Corresponding Author: Dongming.Mei@usd.edu
†Equal contributor:Wenzhao.Wei@usd.edu
‡Equal contributor:Lu.Wang@usd.edu

pendent in which the direct excitation increases with energy decreasing. This implies that, in the low-energy region, the energy response function is not a linear function for a dual-phase xenon detector. Thus, a relative calibration using well-known gamma-ray sources or electron sources above the low energy region can be largely uncertain in determining the energy scale for the low-energy region. This uncertainty can further propagate in the determination of the energy scale for nuclear recoils for a dual-phase xenon detector if a relative calibration is performed. Consequently, the sensitivity limits achieved for WIMPs searches may possess large uncertainty. We propose an absolute energy response function (Eq.(2)) to evaluate this uncertainty.

The determination of α and β using the relationship between E_{real} and E_r is called an absolute energy response function. For a given detector, the variation of ε results in a variation of real energy that can be detected. This variation can be predicted using the following relation:

$$\frac{E_g}{\varepsilon}\frac{dE_{vis}}{dx} = \frac{\alpha}{1+\beta\frac{dE_{eff}}{dx}}\frac{dE_{eff}}{dx}. \quad (3)$$

In the case of a germanium detector at 77 Kelvin, ε = 2.96 eV and the variation of ε is negligible. Therefore, we predict $\alpha = (0.249\pm0.013)$ and $\beta = (5.12\pm2.68)\times10^{-5}$ cm/MeV and these values are verified using experimental data [24]. However, for a liquid xenon detector, the observable quanta are scintillation photons, which are produced through direct excitation and recombination of electron-ion (e-ion) pairs from ionization. Thus, the average energy expended per e-ion pair varies as a function of the ratio of direct excitation to ionization per energy deposition process, $\varepsilon = (1.13 + 0.9\frac{N_{ex}}{N_i} + 0.48)E_g$ [25]. The ratio of direct excitation to ionization can be described as a function of deposition energy [26]:

$$\frac{N_{ex}}{N_i} = \frac{1-exp(-\frac{I}{E})}{exp(-\frac{I}{E})}, \quad (4)$$

where I is the mean ionization potential and E is the deposition energy. For xenon, I= 35.55 + 9.63Z [27], where Z=54. As can be seen in Eq.(4), when E = 1 keV, $\frac{N_{ex}}{N_i}$ = 0.74 while E = 10 keV, $\frac{N_{ex}}{N_i}$ = 0.057. Plugging Eq.(4) into $\varepsilon = (1.13 + 0.9\frac{N_{ex}}{N_i} + 0.48)E_g$, one obtains ε. Using Eq.(3), we determine $\alpha = (0.74\pm0.04)$ and $\beta = (6.57\pm1.1)\times10^{-3}$ cm/MeV for liquid xenon at 165 Kelvin. These values are compared to the values obtained with data [28] and a reasonable agreement was achieved. With these parameters, we obtain the absolute ionization efficiency of nuclear recoils for a germanium detector and the absolute scintillation efficiency of nuclear recoils for a liquid xenon detector at zero field as shown in Figure 1. Utilizing Eq.(2) and Eq.(3), a dual-phase liquid xenon detector with 3 photoelectrons detected at an efficiency of 14% in liquid and 50 photonelectrons detected in gas with a multiplication factor of 24.55 and an extraction efficiency of 65% would correspond to a detection threshold energy of 6.8 keV nuclear recoil energy [28].

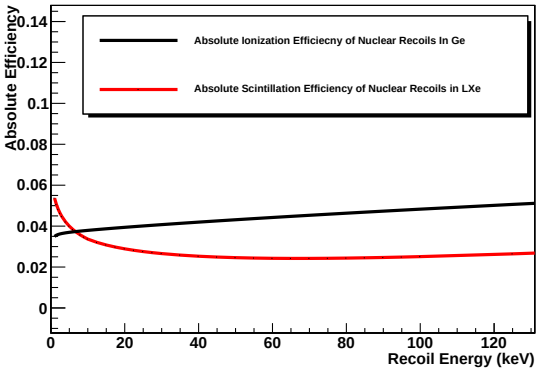

FIG. 1: The absolute efficiency of nuclear recoils for liquid xenon at zero field and germanium detectors.

The discrimination of nuclear recoils from electronic recoils is usually performed through a well-defined nuclear recoil band and electronic recoil band for a given technology such as dual-phase liquid xenon detectors [29, 30] and cryogenic germanium detectors at 50 mini-Kelvin [31, 32]. The width of bands is given by the respective energy resolution of nuclear recoils and electronic recoils for a given detector. All experiments treat energy resolution the same for both nuclear recoils and electronic recoils. This is only valid if electronic noise and incomplete charge are dominant contributions to the energy resolution while the intrinsic statistical variation is negligible for a given detector. However, for a dual-phase liquid xenon detector and a germanium detector, the intrinsic statistical variation either dominates the detector energy resolution or is comparable to the contributions from electronic noise and incomplete charge. For example, XENON100 [33] reported the following energy resolution functions: (1) $\frac{\sigma(E)}{E} = (\frac{1.0}{\sqrt{E/MeV}} + 11.2)\%$ for S1 only, (2) $\frac{\sigma(E)}{E} = (\frac{2.4}{\sqrt{E/MeV}} + 3.5)\%$ for S2 only, and (3) $\frac{\sigma(E)}{E} = \frac{1.9\%}{\sqrt{E/MeV}}$ for combined S1 and S2. These three cases can be described by an energy dependence of the resolution $\frac{\sigma(E)}{E} = \frac{c_1}{E} + c_2$. It is clear that $\frac{c_1}{E}$ is related to the statistical variation and c_2 describes the noise level. Note that c_2 is comparable to zero for combined S1 and S2 reported by XENON100 [33]. This implies that the statistical variation dominates the energy resolution of the XENON100 detector for the case of combined S1 and S2. In the case of the CDMS experiment, the detector-averaged energy resolution below 10 keV was reported to be $\sigma(E) = \sqrt{(0.293)^2 + (0.056)^2 E[keV]}$ [34]. As can be seen in this equation, the term, $(0.293)^2$, is related to the contribution from noise and incomplete charge, and the term, $(0.056)^2 E$ represents statistical variation. The contributions from these two terms are comparable. In the case in which the statistical variation dominates the energy resolution or is comparable to the contribution from noise and incomplete charge, the energy resolution

for nuclear recoils cannot be described by the measured energy resolution with gamma-ray sources. This is because the statistical variation of nuclear recoils events differs from that of electronic recoil events with the same energy. We attribute this difference to the processes of energy partition for these two classes of events.

Upon deposition of energy in a given target, E_0, two types of excitations, (a) lattice excitation with no formation of mobile charge pairs and (b) ionization with formation of mobile charge pairs, are created by an incoming particle. Lattice excitations produce N_x phonons of energy E_x. Ionization form N_i charge pairs of energy E_i. For an energy loss process, energy conservation requires $E_0 = E_i N_i + N_x N_x$. As fluctuations in N_i are compensated by fluctuations in N_x to keep E_0 constant, $\frac{dE_0}{dN_i}\Delta N_i + \frac{dE_0}{dN_x}\Delta N_x = 0$ and $E_i \Delta N_i + E_x \Delta N_x = 0$. From averaging many events, one obtains for the variance: $E_i \sigma_i = E_x \sigma_x$, with $\sigma_x = \sqrt{N_x}$ assuming Gaussian statistics. Thus, $\sigma_i = \frac{E_x}{E_i}\sqrt{N_x}$. Since $N_x = \frac{E_0 - E_i N_i}{E_x}$, one obtains $\sigma_i = \frac{E_x}{E_i}\sqrt{\frac{E_0}{E_x} - \frac{E_i}{E_x}N_i}$. Each ionization leads to a charge pair that contributes to the signal, therefore, $N_i = \frac{E_0}{\varepsilon_i}$ and

$$\sigma_i = \sqrt{\frac{E_0}{\varepsilon_i}} \cdot \sqrt{\frac{E_x}{E_i}(\frac{\varepsilon_i}{E_i} - 1)}, \tag{5}$$

where ε_i represents mean energy expended per e-h pair.

The statistical variation is usually quantified by the Fano factor [35] (F), which is defined for any integer-valued random variable as the ratio of the variance (σ_i^2) of the variable to its mean (N_i), $F = \frac{\sigma_i^2}{N_i}$. Thus, one obtains $\sigma_i = \sqrt{F N_i}$. Comparing this expression to Eq. (5), one finds

$$F = \sqrt{\frac{E_x}{E_i}(\frac{\varepsilon_i}{E_i} - 1)}, \tag{6}$$

In the case of the SuperCDMS-like detector, the average energy expended per e-h pair, ε, is critical to interpret the measured phonon energy and hence the measured recoil energy since $E_r = E_p$ - $E_Q \frac{eV_b}{\varepsilon}$ is used to reconstruct recoil energy, where E_p the measured phonon energy, E_Q the ionization energy, and V_b the bias voltage. However, there are several processes [36] that reduce phonons. Therefore, the measured phonon energy must be corrected for efficiencies, $E_p = \eta_{pri}(E_r - \frac{E_Q}{\varepsilon}E_g) + \eta_{rec}(f_Q \frac{E_Q}{\varepsilon})E_g + \eta_{Luke}(f_Q \frac{E_Q}{\varepsilon} eV_b)$, where η_{pri}, η_{rec}, and η_{Luke} the detection efficiencies for primary phonons, the phonons from recombination of e-h pairs, and Luke phonons, respectively, and f_Q the fraction of the total charge observed. Because of such a complicated relation of the measured phonon energy with different efficiencies, ε has to be determined independently. At 50 mini-Kelvin, the average primary phonon energy is about 8.282×10^{-3} eV with a frequency of 2 THz [37]. The Neganov-Luke phonons have an average energy of 1.242×10^{-3} eV with a frequency of 0.3 THz [38]. The band gap energy at

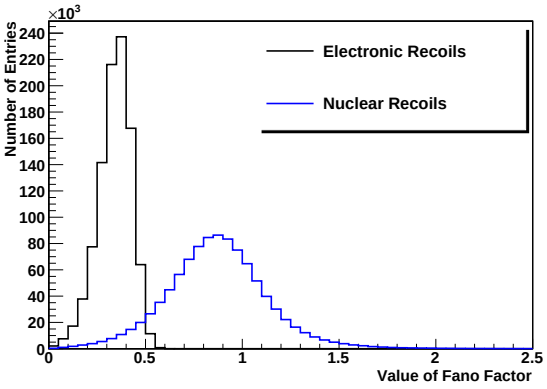

FIG. 2: The calculated Fano factors for electronic recoils and nuclear recoils in germanium detector at 50 mini-Kelvin.

50 mini-Kelvin is about 0.742 eV. Using Eq.(6) and the measured energy resolution related to statistical variation, $(0.056)^2$E(keV) [34], one obtains a Fano factor, F = 0.35 and ε_{ER} = 8.9 eV (depending on the average primary phonon energy) at 50 mini-Kelvin for electronic recoils. The average energy expended per e-h pair for nuclear recoils can be expressed as $\varepsilon_{NR} = \frac{\varepsilon_{ER}}{\varepsilon}$, where ε is ionization efficiency, which can be calculated using Lindhard's theory [7] or Barker-Mei's model [40, 41]. Together with Eq.(6), the Fano factor for nuclear recoils can be obtained as shown in Figure 2. Note that the ionization yield for electronic recoils is normalized to be a unit. If one uses ε_{ER} = 8.9 eV instead of 3 eV [31] in a SuperCDMS-like detector, the threshold of nuclear recoil energy is determined to be ∼4.5 keV [24] with 50 mini-Kelvin at 69 volts. As can be seen in Figure 2, the Fano factor for low energy electronic recoils is a sub-Poisson distribution, while the Fano factor for nuclear recoils is a convolution of both sub-Poisson (Fano factor < 1) and super-Poisson (Fano factor > 1) distribution depending on nuclear recoil energy. Consequently, the width of nuclear recoils and the width of electronic recoils using the ratio of ionization yield to the total phonon energy are governed by the intrinsic statistical variation of these two classes of events as shown in Figure 3. In the generation of Figure 3, the electronic recoils were randomly chosen between 0.1 keV to 100 keV, while the nuclear recoils were simulated with ^{252}Cf neutron energy spectrum expressed as $N(E_n) = \sqrt{E_n} e^{(-E_n/1.565)}$ [42]. It is demonstrated in Figure 3 that there is no discrimination between electronic recoils and nuclear recoils when the phonon energy (recoil energy) is below 2 keV. The energy resolution, $\sigma(E)$, induced by this statistical variation for the 2 keV nuclear recoil is about 0.3 keV. Note that the $\sigma(E)$ for the 0.5 keV and 2 keV electronic recoil is about 0.037 and 0.085 keV, respectively. Therefore, the uncertainty on the threshold energy of nuclear recoils must be evaluated separately from electronic recoils.

For a given dual-phase xenon detector, the Fano factor for optical photons is $F_N = \sigma_N^2/\bar{N}$. This value was

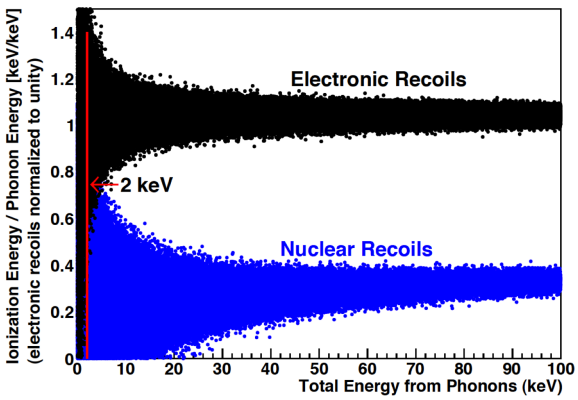

FIG. 3: The predicted electronic recoil band and nuclear recoil band for a germanium detector at 50 mini-Kelvin. The red line stands for 2 keV phonon energy.

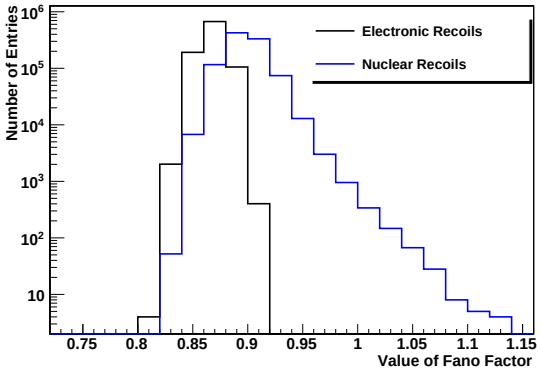

FIG. 4: The calculated Fano factors for electronic recoils and nuclear recoils in liquid xenon detector at 165 Kelvin.

measured to be 0.059 by Doke et al. [43]. Since liquid xenon detectors detect optional photons with photomultipliers, which convert optical photons into photoelectrons. Therefore, the Fano factor for the photoelectrons becomes, $F_n = \sum_{i=1}^{n}(1 + \epsilon(F_N - 1)$ [44], where i runs from 1 to the number of photomultipliers that are fired per event, ϵ is the probability that an optical photon will reach the photo-detector and produce a photoelectron. If one assumes $\epsilon = 0.14$ [30], the Fano factor for photoelectrons is about 0.87 for electronic recoils with one photomultiplier. Using Eq.(6), one can determines $E_x = 0.047$ eV if the average energy expended per electron-hole pair, $\varepsilon = 15.6$ eV [45]. Thus, we can determine Fano factor for nuclear recoils using the similar method described above. Figure 4 shows Fano factor for electronic recoils and nuclear recoils in liquid xenon with one photomultiplier. Depending on the number of photomultipliers that are involved in detecting photons from an energy deposition, the Fano factor can be much larger than 1.

As a result, the statistical variation dominates the widths of the nuclear recoil band and the electronic recoil

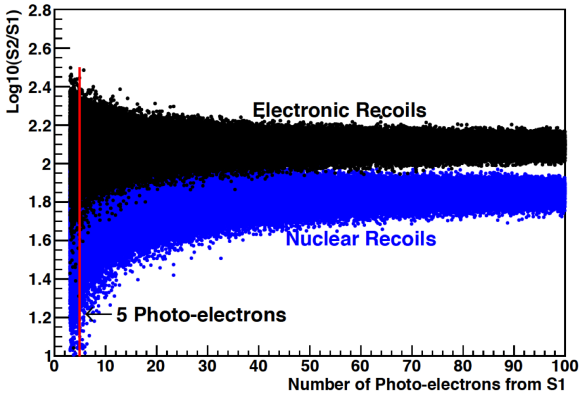

FIG. 5: The predicted electronic recoil band and nuclear recoil band for a dual-phase liquid xenon detector at 165 Kelvin without considering the saturation effect in S2. The red line represents 5 photoelectrons, which corresponds to 3.5 keV nuclear recoil energy.

band using the ratio of signal in gas phase (S2) to signal in liquid (S1) for discriminating these two classes of events as shown in Figure 5. In the simulation of S1 and S2 signals, we assume the product of photon detection efficiency and the photoelectron efficiency is 14% [30] in liquid, the electron extraction efficiency from liquid to gas phase is 65% [30], and the photon multiplification factor of S2 is 24.55 [30]. Note that the saturation effect in S2 was not taken into account in the simulation.

As can be seen in Figure 5, when photoelectrons in S1 is less than 2, which represents about 1.5 keV, the dual-phase xenon detector loses the discrimination power. At a 3 keV nuclear recoil energy, the energy resolution, $\sigma(E)$, is about 0.7 keV while $\sigma(E)$ is about 0.3 keV for the 2 keV and 0.1 keV for the 0.9 keV electronic recoils.

In conclusion, the absolute energy response functions with two parameters, α and β, describe the energy scale for electronic recoils and nuclear recoils. The values of α and β can be calculated or determined using well-known gamma ray sources. The Fano factor for nuclear recoils dominates the energy resolution in the low energy region for detecting WIMPs using both SuperCDMS-type and dual-phase xenon detectors. The Fano factor for nuclear recoils is larger than that of electronic recoils. Note that the difference in Fano factors between nuclear recoils and electronic recoils is mainly due to the difference in the average energy expended per e-h pair. This causes a different energy scale function between nuclear recoils and electronic recoils. Therefore, the calibration of both energy scale and energy resolution needs to be implemented for electronic recoils and nuclear recoils separately.

The authors wish to thank Christina Keller for careful reading of this manuscript. This work was supported in part by NSF PHY-0919278, NSF PHY-1242640, DOE grant DE-FG02-10ER46709, and a governor's research center supported by the state of South Dakota.

[1] F. Zwicky, Helv. Phys. Acta 6 (1933) 110-127.
[2] G. Hinshaw et al. (WMAP Collaboration), ArXiv: 1212.5226, APJS 208 (2013) 19.
[3] R. J. Gaitskell, Ann. Rev. Nucl. Part. Sci. 54 (2004) 315-359.
[4] L. Evans and P. Bryant (Eds.), LHC Machine, JINST 3 (2008) S08001.
[5] J. L. Feng, Supersymmetry and Cosmology, Annals of Physics 315, Issue 1 (2005) 2-15, arXiv:hep-ph/0405215.
[6] M. W. Goodman and E. Witten, Detectability of certain dark-matter candidates, Phys. Rev. D 31 (June, 1985) 3059-3063.
[7] J. Lindhard et. al., Mat. Fys. Medd. K. Dan. Vidensk. Selsk. 33, 1 (1963).
[8] D.-M. Mei et al. Astroparticle Physics 30 (2008) 12-17.
[9] J. B. Birks, Proc. Phys. Soc. A64 (1951) 874. J.B. Birks (1964), The Theory and Practice of Scintillation Counting. London: Pergamon.
[10] E. Aprile et al., Phys. Rev. D 86, 112004 (2012).
[11] L. Baudis, H. Dujmovic, C. Geis, A. James, A. Kish, A. Manalaysay, T. Marrodn Undagoitia, and M. Schumann, Phys. Rev. D 87, 115015 (2013).
[12] J. Thomas and D. A. Imel, Phys. Rev. A 36, 614 (1987).
[13] M. Miyajima, T. Takahashi, S. Konno, T. Hamada, S. Kubota, H. Shibamura, and T. Doke, Phys. Rev. A 9, 1438 (1974).
[14] T. Doke, A. Hitachi, J. Kikuchi, K. Masuda, H. Okada, and E. Shibamura, Jpn. J. Appl. Phys. 41, 1538 (2002).
[15] E. Aprile, K. L. Giboni, P. Majewski, K. Ni, and M. Yamashita, Phys. Rev. B 76, 014115 (2007).
[16] Wei Mu, Xiaonu Xiong, Xiangdong Ji, Astropart.Phys. 61 (2015) 56-61.
[17] A. Manzur, A. Curioni, L. Kastens, D. N. McKinsey, K. Ni, T. Wongjirad, Physical Review C, vol. 81, Issue 2 (2010) 025808.
[18] B. Lenardo et al., arXiv: 1412.4417.
[19] J. Mock et al., JINST 9 (2014) T04002, arXiv: 1310.1117.
[20] M. Szydagis et al., JINST 8 (2013) C10003, arXiv: 1307.6601.
[21] M. Szydagis et al., JINST 6 (2011) P10002, arXiv: 1106.1613.
[22] F. E. Emery and T. A. Rabson, Phys. Rev. 140 (1965) 2089.
[23] J.M.F. dos Santos, C.M.B. Monteiro, Applied Radiation and Isotopes 55 (2001) 331.
[24] W.-Z. Wei, L. Wang, D.-M. Mei, in preparation.
[25] T. Takahashi et al., Phys. Rev. A 12 (1975) 1771.
[26] Saha, Megh Nad (1920). "LIII.Ionization in the solar chromosphere". Philosophical Magazine Series 6 40 (238): 472.
[27] Shankar Mukherji, Phys. Rev. B 9 (1975) 3530.
[28] L. Wang, W.-Z. Wei, D.-M. Mei, in preparation.
[29] E. Aprile et al. (XENON100 Collaboration), Phys. Rev. Lett. 109, 181301 (2012). arXiV: 1207.5988.
[30] D. S. Akerib et al. (LUX Collaboration), Phys. Rev. Lett. 112, 091303 (2014). arXiv:1310.8214.
[31] R. Agnese et al. (SuperCDMS Collaboration), Phys.Rev.Lett. 112 (2014) 241302.
[32] E. Armengaud et al. (EDELWEISS Collaboration) Phys. Lett. B 702 (2011) 329-335.
[33] E. Aprile et al. (XENON100 Collaboration), Astropart. Phys. 35 (2012), 573-590.
[34] Z. Ahemd et al. (CDMS Collaboration), Phys. Rev. D 81, 042002 (2010).
[35] U. Fano, Phys. Rev. 72 (1947) 26.
[36] Scott M. Fallows, PhD thesis dissertation, University of Minnesota, December, 2014.
[37] Scott A. Hertel (SuperCDMS Collaboration) PhD thesis "Advancing the Search for Dark matter: from CDMS II to SuperCDMS", http://cdms.berkeley.edu/Dissertations/hertel.pdf.
[38] G. Wang, Journal of Applied Physics 107, 094504 (2010).
[39] F. E. Emery and T. A. Rabson, Phys. Rev. 140 (1965) A2089.
[40] D. Barker and D.-M. Mei, Astroparticle Physics, Volume 38, p. 1-6. arXiv:1203.4620v4.
[41] D. Barker et al., Astroparticle Physics, Volume 48, p. 8-15. arXiv:1304.6773.
[42] J. W. Meadows, Phys. Rev. 157 (1967) 1076.
[43] T. Doke, et al., 1976, Nucl. Instrum. Methods 134, 353.
[44] Abdelkader Bousselham, Harrison H.Barrett, Vaibhav Bora and Kanai Shah, Nucl. Instrum. Methods in Phys. A 620 (2010) 359 - 362.
[45] E. Aprile and T. Doke, Reviews of Modern Physics, V 82, JULYSEPTEMBER 2010.